

# Personalized Video Relighting With an At-Home Light Stage

Jun Myeong Choi, Max Christman, Roni Sengupta

University of North Carolina at Chapel Hill



Figure 1. We use our Light Stage at Your Desk (LSYD) dataset to build a personalized relighting algorithm that generates temporally consistent and high-quality portrait videos under different lighting conditions. This data could easily be captured at home, as it just consists of recordings of users while watching videos at a monitor. We used background matting [16] to replace the original background with a portion of the environment map.

## Abstract

In this paper, we develop a personalized video relighting algorithm that produces high-quality and temporally consistent relit videos under any pose, expression, and lighting condition in real-time. Existing relighting algorithms typically rely either on publicly available synthetic data, which yields poor relighting results, or instead on light stage data which is difficult to obtain. We show that by just capturing video of a user watching YouTube videos on a monitor we can train a personalized algorithm capable of performing high-quality relighting under any condition. Our key contribution is a novel neural relighting architecture that effectively separates the intrinsic appearance features — the geometry and reflectance of the face — from the source lighting and then combines them with the target lighting to generate a relit image. This neural network architecture enables smoothing of intrinsic appearance features leading to temporally stable video relighting. Both qualitative and quantitative evaluations show that our architecture improves portrait image relighting quality and temporal consistency over state-of-the-art approaches on both casually captured ‘Light Stage at Your Desk’ (LSYD) and light-stage-captured ‘One Light At a Time’ (OLAT) datasets.

## 1. Introduction

With the recent rise in popularity of video conferencing for business, educational, and personal activities, there is a significant demand for improving facial lighting. Virtually relighting our images and videos helps us to improve the

appearance of our faces without requiring explicit studio-quality lighting in a dedicated space or any specialized lighting expertise. Recent advances in deep neural networks have renewed interest in the problem of virtual relighting.

Training a deep neural network for relighting requires extensive training data that includes source images paired with relit target images. One way of acquiring this data is by using a large spherical rig with numerous lights and cameras, known as a light stage [3]. While light stage data has been shown to produce high-quality relighting results [18, 19, 28, 29, 34, 37], the limited availability of datasets, trained models, and access to the light stage itself has impeded further research. For example, *One Light At a Time* (Dynamic-OLAT) [34] is the only publicly available light stage relighting dataset consisting of four individuals only. As a result, researchers have often turned to synthetic data to train their relighting algorithms [9, 22, 27, 39]. Unfortunately, existing synthetic data compromises the quality of relit images.

We draw inspiration from recent work by Sengupta *et al.* [23] and develop a personalized relighting model by capturing a single user’s appearance while lit by a computer monitor. While their casually captured data showed early promise, it fails to generalize for several reasons. First, it requires capturing users with fixed poses and expressions, an unrealistic requirement for actual users. Second, the relighting algorithm requires knowledge of the source lighting, limiting it to images captured in front of a monitor in a dimly lit room. Additionally, the resulting relit video is tem-

porally unstable, exhibiting significant flickering artifacts. Their algorithm frequently produces unsatisfactory results when applied to faces captured in challenging lighting conditions. These limitations prevent Sengupta *et al.* [23] from producing stable and high-quality relighting under any arbitrary pose, expression, and lighting conditions.

In this paper, we show that casually captured light stage data is sufficient to develop a high-quality temporally consistent video portrait relighting algorithm that can relight a user’s face captured under arbitrary conditions (i.e. pose, expression, and ambient lighting) in real-time. To that end, we create our own casually captured light stage dataset with varying pose, expression, and lighting, called *Light Stage at Your Desk* (LSYD). Our key contribution is a neural relighting architecture, based on the commonly used U-Net [18, 28, 29, 31, 39], that disentangles the source lighting from the user’s intrinsic facial appearance (shape and reflectance) and then adds back the target lighting to generate a relit image. To this end, we introduce the *light-conditioned feature normalization* (LCFN) module, which does relighting and also predicts the source lighting from an input image. The LCFN module also enables temporal stability by performing exponential smoothing of *de-lit* intrinsic appearance features. We also improve the data pre-processing pipeline from Sengupta *et al.* [23] to make the relighting algorithm more robust to pose, expression, and ambient lighting conditions. Our proposed relighting framework is general and can relight any portrait image with unknown source lighting by predicting the source lighting and using it for de-lighting with the LCFN module.

We compare our relighting network with two other algorithms: Sun *et al.* [28], which was originally trained on light stage data (OLAT), and Sengupta *et al.* [23], which was originally trained on casually captured data (albeit with fixed pose, expression, and ambient lighting). For a fair comparison, we train all algorithms for personalized relighting using the same data pre-processing steps and loss functions on 5 individuals from our LSYD dataset and 4 individuals from OLAT [34]. Our network outperforms Sun *et al.* [28] and Sengupta *et al.* [23] by 22.3% and 23.6% respectively on the LSYD dataset and by 23.5% and 25.6% on the OLAT dataset, in terms of LPIPS. Qualitatively our method produces superior relighting in terms of color, quality, and consistency. We further show that our approach is more temporally consistent, leading to less flickering than Sun *et al.* [28] or Sengupta *et al.* [23]. Detailed ablation studies show that LCFN and source monitor prediction improves relighting quality, feature and source monitor smoothing improves temporal consistency, and data pre-processing improves robustness to pose and expression.

To summarize, our main contributions are as follows:

- We show that casually captured *Light Stage at Your Desk* (LSYD) data can be used to build a high-quality tempo-

rally consistent personalized video relighting algorithm without requiring access to an expensive light stage setup.

- We introduce a novel video relighting architecture that separates the source lighting from the user’s intrinsic appearance features and then adds back the target lighting, leading to improved relighting and temporal consistency of for videos.
- We show that our relighting architecture is universal, achieving state-of-the-art performance on both the LSYD and light stage-captured OLAT [34] datasets. Our network can relight any portrait image in an arbitrary pose, expression, and lighting conditions.

## 2. Related work

Portrait relighting methods change the appearance of the face to match a target lighting condition. This can be expressed through lighting parameters, e.g. an environment map, spherical harmonics, directional lighting, etc.) or through a reference image of another person. Our approach relights a portrait image to a lighting condition expressed through a low dynamic range image representing the image on the monitor.

**Reference image-based relighting.** Shu *et al.* [26] introduced a face relighting approach that uses a mass-transport formulation for the transfer of illumination between images. Peers *et al.* [20] demonstrated a method for relighting portrait images with flat lighting to match specific target environments, incorporating a reference subject database for approximation. Shih *et al.* [25] adopted a multiscale technique to transfer local image statistics from reference portraits onto new ones, facilitating the matching of attributes like local contrast and overall lighting direction.

**Learning from synthetic data.** Recent advancements in deep learning have caused significant shifts to the landscape of portrait relighting. These deep learning approaches often rely on synthetic data to learn relighting. Some studies [15, 22, 32] create a virtual relighting dataset by using synthetic human models to train their networks. In contrast, others [2, 9, 10, 39] generate relit images by using public datasets and employ methods based on ratio images or 3D model rendering. Specifically, Zhou *et al.* [39] and Hou *et al.* [9] make use of spherical harmonics and ratio images for relighting. Furthermore, Hou *et al.* [10] takes a more advanced approach by introducing explicit components, where rays originating from the face intersect with other parts of the facial geometry to create relit images. However, when using synthetic data to train a neural network, the large domain gap between synthetic and real data impacts the model’s performance on real data.

**Learning from light stage data.** The extensive use of light stages [3] for data collection has enabled numerous innovative studies [5, 8, 17–19, 28, 29, 33, 38] in this domain. Some researchers have incorporated explicit elements such as albedo, normals, specular maps, and diffuse maps into

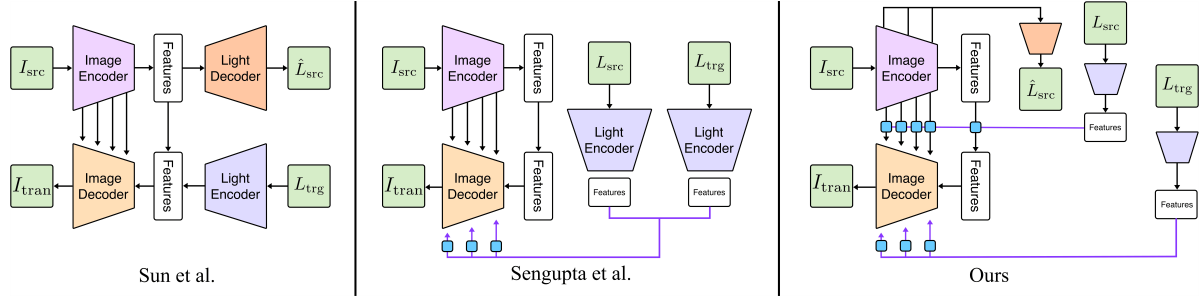


Figure 2. We highlight the key structural differences between our relighting architecture to that of [23, 28]. Our approach remove source lighting information from input image features and only propagates intrinsic appearance (geometry and reflectance) features from encoder to decoder, which results in better relighting quality and more temporal stability. In contrast [23, 28] propagates entire image features from encoder to decoder without ‘delighting’, and expects the decoder to remove source lighting and add target lighting information.

their methodologies [5, 18, 19, 31]. Others have taken a physics-based rendering approach [8, 33] to resolve these issues. Other papers aim to manipulate lighting conditions and generate images under different lighting scenarios using texture information [17, 34, 38]. Recent works have instead embraced an intrinsic approach [28, 29], enabling neural networks to directly and inherently handle the relighting process. However, these approaches typically utilize light-stage captured data, which are not publicly available and are expensive to capture. In contrast, recent studies aim to streamline the capture process, using a mobile phone camera [24] or a sun stage [30] instead of a light stage. Nevertheless, due to their reliance on optimization, both of these papers lack the capability for real-time relighting. Instead, our approach builds a personalized relighting algorithm using casually captured videos from the desk recording setup introduced in Sengupta *et al.* [23]. Our algorithm also performs intrinsic relighting, similarly to [23, 28, 29], and improves the relighting quality compared to [23, 28], enabling real-time temporally consistent video relighting under any pose, expression and ambient lighting.

### 3. Method

Our setup is similar to Gerstner *et al.* [7] and Sengupta *et al.* [23], where a user’s face is captured while illuminated by their monitor. By capturing multiple videos of the user’s face along with the video on their monitor, we build our ‘at home’ light stage dataset. We then use these data to train a personalized portrait relighting algorithm that can render the user’s face under arbitrary lighting conditions. Specifically, given a portrait image  $I_{src}$ , corresponding source monitor lighting  $L_{src}$ , and target monitor lighting  $L_{trg}$ , our aim is to learn a function  $G$  that relights  $I_{src}$  under  $L_{trg}$ :

$$\hat{I}_{trg}, \hat{L}_{src} = G(I_{src}, L_{src}, L_{trg}; \theta_G). \quad (1)$$

Note that our formulation can be used for scenarios where the source lighting is unknown by simply replacing the input source lighting with the predicted source lighting, unlike previous approaches [23].

In the following sections, we outline our methodology for portrait video relighting using a monitor as a light stage. Section 3.1 outlines strategies for constructing training data pairs from casually captured videos that allow flexibility in facial expression, pose, and ambient lighting. In Sec. 3.2, we introduce our relighting network architecture that disentangles lighting from intrinsic appearance using light-conditioned feature normalization, leading to high-quality relit images. In Sec. 3.3, we propose additional techniques which enforce temporal consistency and eliminate flickering, also using LCFN. Finally, in Sec. 3.4, we discuss how to train our relighting network.

#### 3.1. Constructing training data pairs

While past work [23] imposed requirements of a neutral pose, expression, and dimly lit room, we loosen these constraints to allow subjects in any pose, expression, or ambient lighting conditions. The only constraint we maintain is that the room lighting shall not overpower the light emitted from the monitor. For example, if the capture occurs in front of a window with bright sunlight, the light from the monitor will have minimal impact on the facial appearance of the subject.

As in Sengupta *et al.* [23], we aim to generate source and monitor image pairs  $(I_{src}, L_{src})$ , as well as target image and target monitor pairs  $(I_{trg}, L_{trg})$ , such that we can train our network to produce  $\hat{I}_{trg}$  where  $I_{trg}$  is the ground truth. However, due to unrestricted subject movement during data collection, there is a lack of pixel-aligned data, making random pairs unsuitable. Previous work [23] utilized segmentation for pairing.

However, we observed that segmentation is ineffective at finding pairs of images with the same pose and expression. Thus, we instead use facial keypoint detection [13] to obtain source and target image pairs. Table 3 shows that this simple data pairing approach can improve the relighting quality and robustness with regards to various poses and expressions.

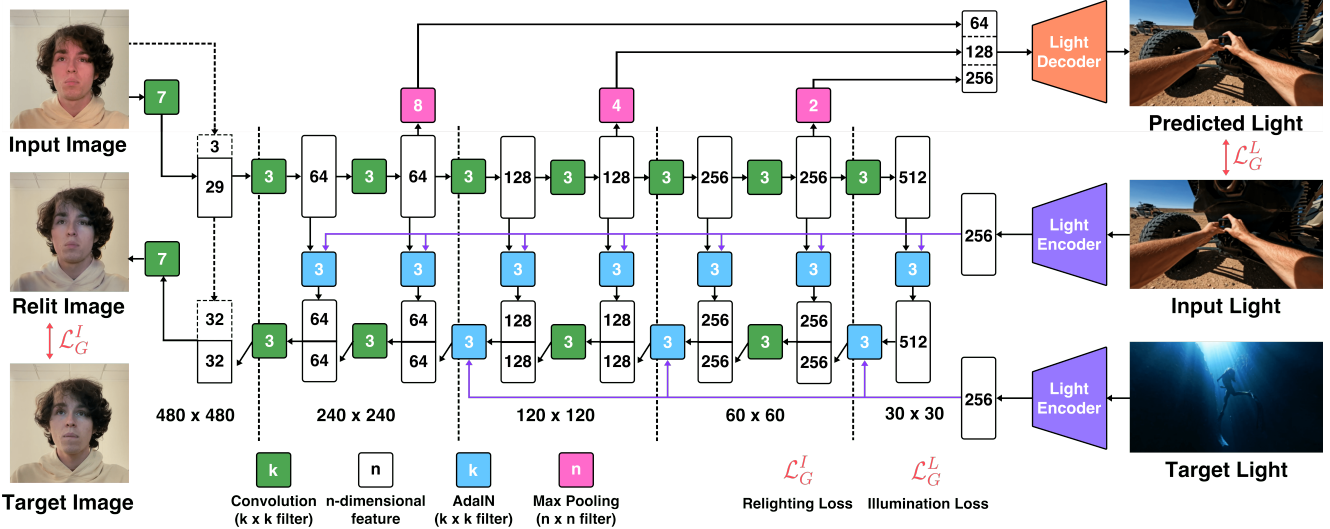


Figure 3. We first de-light the input image features extracted by the U-Net encoder using Adaptive Instance Normalization (AdaIN) guided by the lighting features extracted from the source lighting with a Light Encoder. We then pass these light-normalized encoder features to the decoder of the U-Net and apply another set of AdaIN guided by the features extracted from the target lighting with the Light Encoder. We additionally predict source lighting from the U-Net encoder using a Light Decoder.

### 3.2. Relighting network architecture

Our network architecture, as illustrated in Fig. 3, is built upon the well-established U-Net [21]. This architecture is comprised of a decoder and an encoder with skip connections, which are commonly used in existing portrait relighting algorithms [9, 23, 28, 29, 39].

Our U-Net’s encoder, similar to Sengupta *et al.* [23] and Sun *et al.* [28], processes the source portrait  $I_{\text{src}}$  by applying multiple convolutional layers of varying strides (1 or 2). This process progressively reduces spatial resolution while increasing the number of channels, yielding a latent feature space. The decoder performs the reverse of the encoder by upsampling from the latent features and simultaneously skip connecting to intermediate features from the encoder. These skip connections transport high-frequency shape and appearance information from the encoder to the decoder, ultimately resulting in the generation of a realistic relit image. However, they also carry source illumination features from the encoder to the decoder, leading to subpar relighting quality and temporal flickering. To address this issue, we introduce *light-conditioned feature normalization* (LCFN) for the skip-connected features to better disentangle lighting features from intrinsic appearance features.

To disentangle lighting and intrinsic appearance components from the encoded features – i.e. to de-light – we first predict the source lighting from the encoder features. In contrast to Sun *et al.* [28], which predicts the illumination  $\hat{L}_{\text{src}}$  corresponding to the source image  $I_{\text{src}}$  using the final encoded features, we take a different approach. We extract features at intermediate steps within the encoder, downsample them, and concatenate finally using a confidence learning approach [11] to predict the illumination  $\hat{L}_{\text{src}}$ .

The LCFN module uses the lighting features generated by the lighting encoder to perform Adaptive Instance Normalization (AdaIN) [14] on the encoder features. We begin by using a multi-layer perceptron (MLP) to encode lighting features, transforming the lighting information of  $L_{\text{src}}$  and  $L_{\text{trg}}$  into a compact, low-dimensional representation ( $d = 256$ ). We apply AdaIN to encoder features using the source lighting features, producing normalized features  $f^l$  (for  $l = 1, \dots, 7$ ). Through this normalization process, we induce de-lighting, effectively removing the lighting information present in the encoder features. Starting from the de-lit latent features  $f^7$ , we perform progressive bi-linear upsampling. At each upsampling step, we apply AdaIN to the concatenated feature, incorporating the target lighting features encoded by the lighting encoder. This construction using the LCFN module and source lighting prediction allows us to effectively remove source lighting features from the input and only propagate intrinsic appearance features from the encoder to the decoder. We then add target lighting features in the decoder. The LCFN module also contributes towards temporal consistency (see Sec. 3.3). See Fig. 2 for a comparison between our architecture and those of Sun *et al.* [28] and Sengupta *et al.* [23].

### 3.3. Enforcing temporal consistency

Temporal consistency is vital in making relit videos stable, realistic, and aesthetically pleasing. Previous single-image portrait relighting techniques [23, 28] do not incorporate explicit temporal modeling, leading to undesirable flickering artifacts when applied to videos. Accuracy in single-image portrait relighting can often be uncorrelated to temporal flickering. Inconsistencies across frames are even more no-

ticeable when the source lighting  $L_{\text{src}}$  changes continuously, e.g. watching a video on a Zoom call.

When applied to skip-connected features, LCFN provides a natural defense against temporal flickering by removing source lighting features from the input image. However, it cannot ensure temporal consistency on its own. We notice two further problems: (1) when the source lighting gradually changes, LCFN often leaks small amounts of source lighting information to the decoder, leading to flickering; (2) when source lighting changes abruptly, undesirable fading effects can be observed.

To address this issue, we propose a *skip-connected feature smoothing* technique that assumes neighboring frames share the same intrinsic appearance features, obtained after de-lighting input image features with LCFN. We apply a simple exponential smoothing of de-lit features generated by LCFN, denoted as  $f^l$ , using all the previous frames:

$$f_t^l := \alpha \cdot f_t^l + (1 - \alpha) \cdot f_{t-1}^l \quad (\text{for } l = 1, \dots, 7) \quad (2)$$

with  $\alpha = 0.7$ . Note that exponential smoothing does not work without de-lit LCFN features, which removes time-varying source lighting.

We further notice that when the monitor light changes abruptly there relighting effect is delayed by a few frames, mainly due to the limited refresh rate of the monitor and frame rate of the camera. We thus propose doing a weighted average of source monitor lighting  $L_{\text{src}}$  from a sequence of previous and current frames to achieve smoother and more natural results:

$$L_{\text{src avg}}^t = \frac{\sum_{i=0}^{N-1} \beta^i L_{\text{src}}^{t-i}}{\sum_{i=0}^{N-1} \beta^i}$$

where  $\beta = 0.6$  and  $N = 3$ .

### 3.4. Training relighting network

Our model is trained through minimizing a weighted combination of three loss functions: generator loss, discriminator loss, and monitor loss. The first loss aims to minimize the discrepancies between the true target image  $I_{\text{trg}}$  in our dataset and the predicted target relit image  $\hat{I}_{\text{trg}}$ , leading to accurately relit images. We adopted our generator loss (Eq. 3) and our discriminator loss (Eq. 4) from Sengupta *et al.* [23]:

$$\mathcal{L}_G^I = \lambda_{L1} \mathcal{L}_{L1}(I_{\text{trg}}, \hat{I}_{\text{trg}}) + \lambda_P \mathcal{L}_P(I_{\text{trg}}, \hat{I}_{\text{trg}}) + \lambda_C \mathcal{L}_C(I_{\text{src}}, \hat{I}_{\text{src}}^C) + \lambda_D (D(\hat{I}_{\text{trg}}; \theta_D) - 1)^2, \quad (3)$$

$$\mathcal{L}_D = (D(I_{\text{trg}}; \theta_D) - 1)^2 + (D(\hat{I}_{\text{trg}}; \theta_D))^2, \quad (4)$$

where  $\mathcal{L}_{L1}$  denotes L1 loss,  $\mathcal{L}_P$  denotes perceptual loss [36],  $\mathcal{L}_C$  denotes cycle consistency loss [40], and  $D$  is the discriminator [12].  $\hat{I}_{\text{src}}^C$  and  $\hat{I}_{\text{trg}}^C$  are the outputs from  $G(\hat{I}_{\text{trg}}, L_{\text{trg}}, L_{\text{src}}; \theta_G)$

The monitor reconstruction loss focuses on minimizing the errors between the predicted source light  $\hat{L}_{\text{src}}$  and the true source light  $L_{\text{src}}$  and is expected to enforce improved disentanglement of lighting information from intrinsic appearance features.

$$\mathcal{L}_G^M = \lambda_{L1} \mathcal{L}_{L1}(L_{\text{src}}, \hat{L}_{\text{src}}) + \lambda_P \mathcal{L}_P(L_{\text{src}}, \hat{L}_{\text{src}}) + \lambda_C \mathcal{L}_C(L_{\text{trg}}, \hat{L}_C^{\text{trg}}). \quad (5)$$

Finally, we minimize the image generator loss  $\mathcal{L}_G^I$ , the discriminator loss  $\mathcal{L}_D$ , and the illumination loss  $\mathcal{L}_G^M$  together:

$$\min_{G,D} \mathcal{L}_G^I + \mathcal{L}_D + \lambda_G^M \mathcal{L}_G^M. \quad (6)$$

**Implementation details.** Each portrait image has a resolution of  $480 \times 480$ , and each monitor image is  $18 \times 32$ . The input images are cropped to the subject’s head to limit the effect of the background. For the *light decoder*, we use convolutional layers to maintain a resolution of  $30 \times 30$ , while changing the channel size from  $448 = 256 + 128 + 64$  to  $2304 = 4 \times 18 \times 32$ . Then, we performed  $30 \times 30$  average pooling to downsize the feature map to  $4 \times 18 \times 32$ . Finally, we did a weighted average to obtain a final feature map size of  $3 \times 18 \times 32$ . All convolutional and MLP layers are followed by pixel normalization and a PReLU activation function. We use  $\lambda_{L1} = 1$ ,  $\lambda_P = 0.1$ ,  $\lambda_C = 0.5$ ,  $\lambda_D = 0.1$  and  $\lambda_G^M = 0.5$ . We train the generator and discriminator with the Adam optimizer, with a learning rate of  $10^{-3}$  and  $10^{-6}$ , and a batch size of 2.

## 4. Experiments

In Sec. 4.1, we first discuss our data collection process, which was based on the approach used to compile the Light Stage at Your Desk (LSYD) dataset. In Sec. 4.2, we perform quantitative and qualitative comparisons with existing single-image portrait relighting algorithms and evaluate their temporal consistency. Finally in Sec. 4.3 we perform ablation studies evaluating the effects of data pre-processing and network architecture on relighting performance.

### 4.1. Data

We recorded data from 5 users of diverse ethnicities and genders to ensure a wide range of skin types. Each participant wore a variety of outfits, and we used 4 different ambient lighting conditions per person to mimic the conditions of real-life online meetings. We directed the participants to continuously change their facial expression and pose during the capture sessions. Each user’s face was captured while watching 8 different videos, each 8 minutes long, on different days with varying appearances. We randomly hold out 1 video for testing and use the remaining 7 videos for training. We use this testing sequence only for qualitative evaluation, not for any quantitative metrics. This is because quantitative evaluation requires a pair of source and target

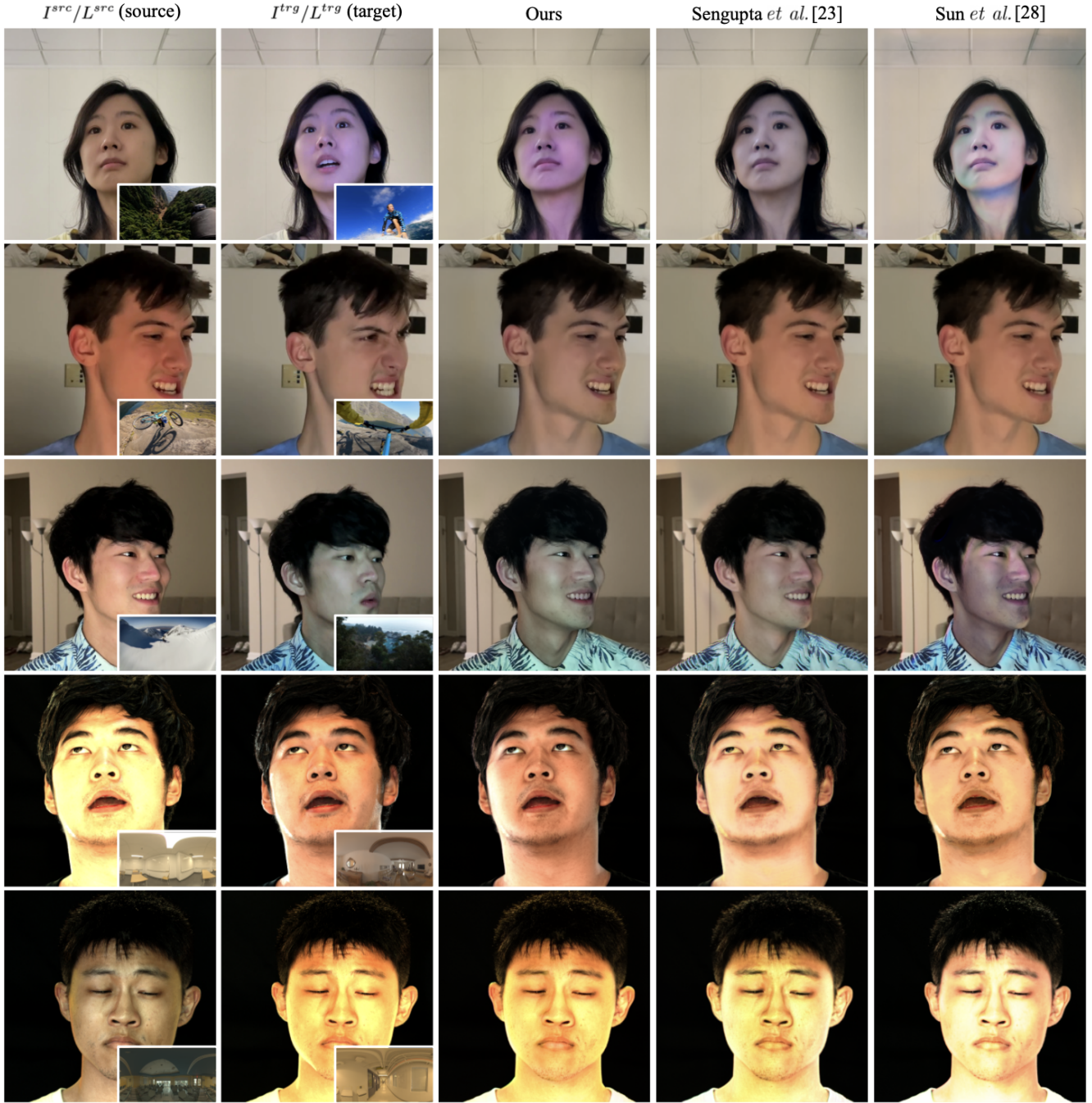


Figure 4. We perform a qualitative comparison with existing relighting techniques [23, 28] on unseen test data both from Light Stage at Your Desk (Rows 1, 2, and 3) and from OLAT [34] (Rows 4 and 5). All models are personalized, i.e. trained on images of that individual only. Our method (Col. 3) produces significantly better relighting results compared to existing approaches (Cols 4 and 5).

images of the same person in the same pose but under different lighting conditions. This is difficult to obtain accurately for the aforementioned test video sequence since the participants naturally vary their pose and expression over the course of the video. Instead, we capture an additional test sequence, used only for numerical evaluation in which the

participant is captured in 9 different pose-expression combinations, each with a distinct monitor light. For each pose, we can create  $\binom{9}{2} = 36$  source and target pairs as input and pseudo ground-truth, resulting in a total of 324 test data pairs per user.

	Known source lighting	LSYD data			OLAT data [34]		
	$L_{\text{src}}$	LPIPS ↓	DISTS ↓	RMSE ↓	LPIPS ↓	DISTS ↓	RMSE ↓
Sun <i>et al.</i> [28] w/ $L_{\text{Sun}}$	–	0.1712	0.1629	8.5958	0.2273	0.1745	6.2692
Sun <i>et al.</i> [28] w/ $L_{\text{Ours}}$	–	0.1029	0.1152	8.4476	0.2267	0.1569	6.1898
Ours	–	0.0839	0.0953	8.3222	0.1812	0.1336	6.0931
Sengupta <i>et al.</i> [23]	✓	0.1018	0.1105	8.2826	0.2237	0.1675	6.1751
Ours	✓	<b>0.0832</b>	<b>0.0953</b>	<b>8.1939</b>	<b>0.1809</b>	<b>0.1334</b>	<b>5.9548</b>

Table 1. We train a personalized relighting model on 5 users from our LSYD dataset and 4 users from the OLAT dataset [34]. We test these models on unseen portrait images and source lighting and report average RMSE, LPIPS [35], DISTS[4] scores on a total of 1620 test images from LSYD and 7172 test images from OLAT. Our method can perform relighting without source lighting  $L_{\text{src}}$ , by simply using the predicted light source from our model as input lighting. Our method significantly outperforms Sun *et al.* [28] and Sengupta *et al.* [23].

## 4.2. Comparison with existing approaches

We employ three error metrics to assess relighting performance: RMSE, LPIPS [36], and DISTS [4]. LPIPS and DISTS are more robust to slight differences in pose between the relit image and the pseudo ground truth and detect perceptual differences more effectively than RMSE.

**Portrait image relighting.** We compared our approach with existing portrait relighting neural architectures — Sun *et al.* [28] and Sengupta *et al.* [23] — by training on our captured LSYD dataset using the same pre-processing for all three architectures (see Sec. 3.1). Our training loss, given in Sec. 3.4, can handle misalignment in source-target pairs in training data, similar to the loss proposed in Sengupta *et al.* [23] (we use an additional loss on source monitor lighting prediction). For Sun *et al.* [28], we train both with their original loss function  $L_{\text{Sun}}$  (which expects perfect source-target pose alignment obtained in OLAT data) and with our proposed loss function  $L_{\text{Ours}}$  to specifically handle misalignment in LSYD data. We train personalized models on 5 users from the LSYD dataset and on 4 users from the publicly available Dynamic OLAT Dataset [34] with 2361 indoor HDR environment lighting maps [1, 6].

For our quantitative evaluation, we test our model on 1620 test images across 5 users with unseen appearance and lighting conditions on the LSYD dataset and on 7172 test images from the Dynamic OLAT dataset. We present the result in Tab. 1. We observe that our proposed approach outperforms Sengupta *et al.* [23] and Sun *et al.* [28] by 22.3% and 23.6% respectively on the LSYD dataset and by 23.5% and 25.6% on the OLAT dataset, when comparing LPIPS score. Our qualitative comparison, as presented in Fig. 4, shows that our model performs superior relighting in terms of color, quality, and consistency.

Note that Sun *et al.* [28] does not require the source lighting  $L_{\text{src}}$  during test time. Our proposed approach can also perform relighting without prior knowledge of source lighting  $L_{\text{src}}$  by simply predicting  $\hat{L}_{\text{src}}$  and using it for light-conditioned feature normalization. We show that even in the absence of  $L_{\text{src}}$ , our method outperforms Sun *et al.* [28] by 22.6% on the LSYD data and by 25.5% on the OLAT

data, in terms of LPIPS. In Figure 5 we demonstrate that our approach can relight any portrait image captured “in-the-wild” without using any monitor light source, and outperforms Sun *et al.* [28].

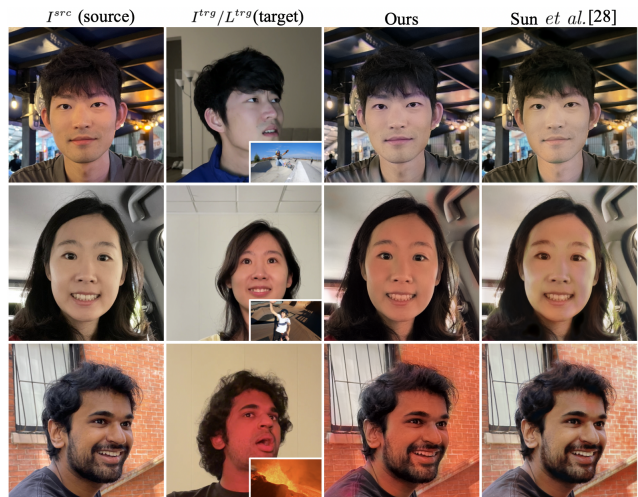


Figure 5. Our method can also relight portrait images captured “in the wild” without using any monitor light source. We can relight a source image (Col. 1) with target lighting shown in the inset in Col. 2. We add a reference of how the user’s face appears under that target lighting in Col. 2 for comparison.

**Portrait video relighting.** Next, we evaluate the temporal consistency of each portrait video relighting algorithm. For each user in the LSYD data, we relit the held-out test video with 50 different target lighting conditions, creating 50 relit videos. We then computed the RMSE between adjacent frames in relit videos as a measure of temporal consistency. Since the pose is almost identical between adjacent frames, lower RMSE error indicates temporally consistent relighting. We then report the average temporal RMSE across all such adjacent frames. In practice, however, a significant fraction of adjacent frame pairs have extremely similar lighting between the two frames, making their relit frames naturally consistent anyway. Only in a small percentage of adjacent frames does the source lighting significantly

	RMSE ↓	Error Rate (%)		
		>0.2	>0.3	>0.4
Threshold		>0.2	>0.3	>0.4
Sun <i>et al.</i> [28]	5.86	13.53	2.61	1.06
Sengupta <i>et al.</i> [23]	6.37	21.83	5.40	1.75
+ $L_{src\_avg}$	5.76	13.31	2.34	0.98
Ours	6.01	16.22	3.61	1.08
+ $L_{src\_avg}$	5.73	13.09	2.31	0.83
+LCFN	5.68	13.04	2.28	0.71
+ $L_{src\_avg}$ +LCFN	<b>5.55</b>	<b>12.89</b>	<b>2.22</b>	<b>0.65</b>

Table 2. We evaluate temporal consistency by relighting a test video with the same target lighting and calculating RMSE between adjacent frames. We then report average RMSE across all adjacent frames and compute an error rate to indicate the percent of adjacent frames with RMSE higher than a threshold.

	Ours		Sengupta <i>et al.</i> [23]	
	LPIPS ↓	DISTS ↓	LPIPS ↓	DISTS ↓
Segment	0.1116	0.1031	0.1229	0.1123
Keypoints	<b>0.0966</b>	<b>0.0932</b>	<b>0.1209</b>	<b>0.1110</b>

Table 3. We observe that keypoint-based source-target data pairing improves upon previous [23] face parsing-based pairing methods.

change, leading to obvious flickering in the relit video if temporal consistency is not maintained. Thus, in addition to average temporal RMSE, we also compute the error rate for three different thresholds: 0.2 (low), 0.3 (medium), and 0.4 (high), which indicate the percentage of adjacent frames where RMSE error is more than a threshold.

In Tab. 2 and Fig. 6, we compare our approach with and without skip-connected feature smoothing to past works [23, 28]. Note that this temporal smoothing of the skip-connected features can only be applied in our framework since we de-light encoder features from the source lighting with LCFN. Both for our approach and for Sengupta *et al.* [23], we can further apply smoothing of input source lighting to handle abrupt changes. We observe that our method produces the most temporally consistent relighting while also being the most accurate (see Tab. 1). We further note that both skip-connected feature smoothing and smoothing of source lighting improve temporal consistency.

### 4.3. Ablation studies

In Sec. 3.1 we discussed how facial keypoint detection, proposed in Sengupta *et al.* [23], enables robustness to relighting with respect to pose and expression, unlike face parsing. This improvement can be seen in Tab. 3.

Next, we remove various components from our relighting network in Tab. 4, specifically the light-conditioned feature normalization and source monitor lighting prediction using intermediate encoder features. We observe that both

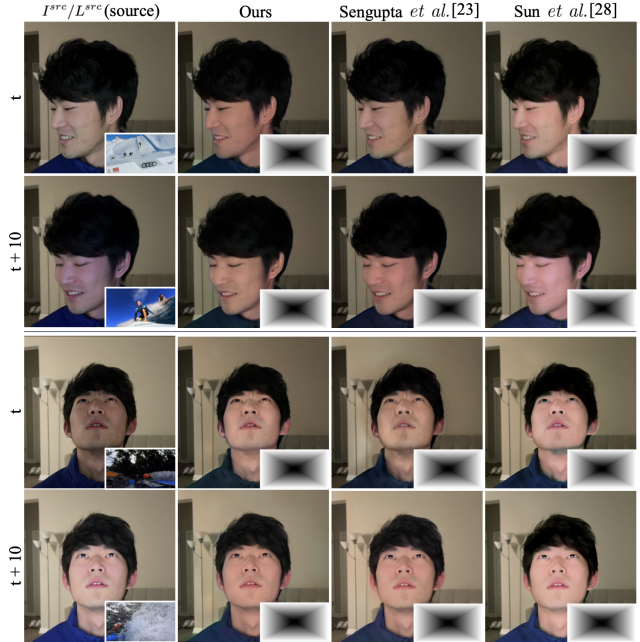


Figure 6. We show temporal consistency between adjacent frames separated by 0.33s by relighting a test video with the same target lighting. Note that [23, 28] both exhibit abrupt changes in lighting between frames  $t$  and  $t + 10$ , while our approach produces a more stable result.

$L_{src}$	de-lighting	RMSE ↓	LPIPS ↓	DISTS ↓
–	–	8.4230	0.0964	0.1071
✓	–	8.2596	0.0915	0.1013
–	✓	8.1907	0.0904	0.0966
✓	✓	<b>8.0746</b>	<b>0.0853</b>	<b>0.0963</b>

Table 4. Both LCFN and source monitor prediction  $L_{src}$  improve relighting performance by effectively disentangling source lighting information from intrinsic appearance features.

improve final relighting performance, which shows their effectiveness in disentangling source lighting information from intrinsic appearance features.

## 5. Conclusion

We propose a personalized video relighting algorithm that leverages casually captured LSYD data to generate real-time high-quality temporally consistent relit videos under any pose, expression, and lighting conditions. We present a novel network architecture that demonstrates excellent performance on both the LSYD and OLAT datasets. While our method performs high-quality facial relighting, it can not change the background lighting since the monitor lighting has minimal effect on the background. Instead, we rely on background matting [16] to effectively replace the background with a part of the environment map.

**Ethical considerations.** While our primary goal is to al-



low people to improve their facial appearance with virtual relighting, we note that it is also a form of image manipulation and can be used for malicious purposes. Further research in detecting forgery via lighting manipulation should be pursued.

**Acknowledgement:** We thank Akshay Pauchuri, Annie Wang, Noah Frahm, Soomin Kim for their support in the data capture process, and in preparation of this manuscript.

## References

- [1] Christophe Bolduc, Justine Giroux, Marc Hébert, Claude Demers, and Jean-François Lalonde. Beyond the pixel: a photometrically calibrated hdr dataset for luminance and color prediction, 2023. 7
- [2] Yuki Endo Daichi Tajima, Yoshihiro Kanamori. Relighting humans in the wild: Monocular full-body human relighting with domain adaptation. *Computer Graphics Forum (Proc. of Pacific Graphics 2021)*, 40(7):205–216, 2021. 2
- [3] Paul Debevec, Andreas Wenger, Chris Tchou, Andrew Gardner, Jamie Waese, and Tim Hawkins. A lighting reproduction approach to live-action compositing. *ACM Trans. Graph.*, 21(3):547–556, 2002. 1, 2
- [4] Keyan Ding, Kede Ma, Shiqi Wang, and Eero P. Simoncelli. Image quality assessment: Unifying structure and texture similarity. *CoRR*, abs/2004.07728, 2020. 7
- [5] David Futschik, Kelvin Ritland, James Vecore, Sean Fanello, Sergio Orts-Escolano, Brian Curless, Daniel Sýkora, and Rohit Pandey. Controllable light diffusion for portraits, 2023. 2, 3
- [6] Marc-André Gardner, Kalyan Sunkavalli, Ersin Yumer, Xiaohui Shen, Emiliano Gambaretto, Christian Gagné, and Jean-François Lalonde. Learning to predict indoor illumination from a single image, 2017. 7
- [7] Candice R. Gerstner and Hany Farid. Detecting real-time deep-fake videos using active illumination. In *2022 IEEE/CVF Conference on Computer Vision and Pattern Recognition Workshops (CVPRW)*, pages 53–60, 2022. 3
- [8] Kaiwen Guo, Peter Lincoln, Philip Davidson, Jay Busch, Xueming Yu, Matt Whalen, Geoff Harvey, Sergio Orts-Escolano, Rohit Pandey, Jason Dourgarian, Danhang Tang, Anastasia Tkach, Adarsh Kowdle, Emily Cooper, Mingsong Dou, Sean Fanello, Graham Fyffe, Christoph Rhemann, Jonathan Taylor, Paul Debevec, and Shahram Izadi. The relightables: Volumetric performance capture of humans with realistic relighting. 2019. 2, 3
- [9] Andrew Hou, Ze Zhang, Michel Sarkis, Ning Bi, Yiyong Tong, and Xiaoming Liu. Towards high fidelity face relighting with realistic shadows. In *IEEE/CVF Conference on Computer Vision and Pattern Recognition (CVPR)*, 2021. 1, 2, 4
- [10] Andrew Hou, Michel Sarkis, Ning Bi, Yiyong Tong, and Xiaoming Liu. Face relighting with geometrically consistent shadows. In *In Proceeding of IEEE Computer Vision and Pattern Recognition*, New Orleans, LA, 2022. 2
- [11] Yuanming Hu, Baoyuan Wang, and Stephen Lin. Fc 4: Fully convolutional color constancy with confidence-weighted pooling. In *Proceedings of the IEEE Conference on Computer Vision and Pattern Recognition*, pages 4085–4094, 2017. 4
- [12] Phillip Isola, Jun-Yan Zhu, Tinghui Zhou, and Alexei A Efros. Image-to-image translation with conditional adversarial networks. *CVPR*, 2017. 5
- [13] Haibo Jin, Shengcai Liao, and Ling Shao. Pixel-in-pixel net: Towards efficient facial landmark detection in the wild. *International Journal of Computer Vision*, 2021. 3

- [14] Tero Karras, Samuli Laine, Miika Aittala, Janne Hellsten, Jaakko Lehtinen, and Timo Aila. Analyzing and improving the image quality of StyleGAN. In *Proc. CVPR*, 2020. 4
- [15] Manuel Lagunas, Xin Sun, Jimei Yang, Ruben Villegas, Jianming Zhang, Zhixin Shu, Belén Masiá, and Diego Gutierrez. Single-image full-body human relighting. *CoRR*, abs/2107.07259, 2021. 2
- [16] Shanchuan Lin, Andrey Ryabtsev, Soumyadip Sengupta, Brian Curless, Steve Seitz, and Ira Kemelmacher-Shlizerman. Real-time high-resolution background matting. *arXiv*, pages arXiv–2012, 2020. 1, 8
- [17] Abhimitra Meka, Rohit Pandey, Christian Haene, Sergio Orts-Escolano, Peter Barnum, Philip Davidson, Daniel Erickson, Yinda Zhang, Jonathan Taylor, Sofien Bouaziz, Chloe Legendre, Wan-Chun Ma, Ryan Overbeck, Thabo Beeler, Paul Debevec, Shahram Izadi, Christian Theobalt, Christoph Rhemann, and Sean Fanello. Deep relightable textures - volumetric performance capture with neural rendering. 2020. 2, 3
- [18] T. Nestmeyer, J. Lalonde, I. Matthews, and A. Lehrmann. Learning physics-guided face relighting under directional light. In *2020 IEEE/CVF Conference on Computer Vision and Pattern Recognition (CVPR)*, pages 5123–5132, Los Alamitos, CA, USA, 2020. IEEE Computer Society. 1, 2, 3
- [19] Rohit Pandey, Sergio Orts-Escolano, Chloe LeGendre, Christian Haene, Sofien Bouaziz, Christoph Rhemann, Paul Debevec, and Sean Fanello. Total relighting: Learning to relight portraits for background replacement. 2021. 1, 2, 3
- [20] Pieter Peers, Naoki Tamura, Wojciech Matusik, and Paul Debevec. Post-production facial performance relighting using reflectance transfer. *ACM Trans. Graph.*, 26(3):52–es, 2007. 2
- [21] Olaf Ronneberger, Philipp Fischer, and Thomas Brox. U-net: Convolutional networks for biomedical image segmentation. *CoRR*, abs/1505.04597, 2015. 4
- [22] Soumyadip Sengupta, Angjoo Kanazawa, Carlos D Castillo, and David W Jacobs. Sfsnet: Learning shape, reflectance and illuminance of faces in the wild. In *Proceedings of the IEEE conference on computer vision and pattern recognition*, pages 6296–6305, 2018. 1, 2
- [23] Soumyadip Sengupta, Brian Curless, Ira Kemelmacher-Shlizerman, and Steven M. Seitz. A light stage on every desk. *CoRR*, abs/2105.08051, 2021. 1, 2, 3, 4, 5, 6, 7, 8
- [24] Artem Sevastopolsky, Savva Ignatiev, Gonzalo Ferrer, Evgeny Burnaev, and Victor Lempitsky. Relightable 3d head portraits from a smartphone video, 2020. 3
- [25] YiChang Shih, Sylvain Paris, Connelly Barnes, William T. Freeman, and Frédo Durand. Style transfer for headshot portraits. *ACM Trans. Graph.*, 33(4), 2014. 2
- [26] Zhixin Shu, Sunil Hadap, Eli Shechtman, Kalyan Sunkavalli, Sylvain Paris, and Dimitris Samaras. Portrait lighting transfer using a mass transport approach. *ACM Trans. Graph.*, 37(1), 2017. 2
- [27] Guoxian Song, Tat-Jen Cham, Jianfei Cai, and Jianmin Zheng. Half-body portrait relighting with overcomplete lighting representation. 2021. 1
- [28] Tiancheng Sun, Jonathan T. Barron, Yun-Ta Tsai, Zexiang Xu, Xueming Yu, Graham Fyffe, Christoph Rhemann, Jay Busch, Paul E. Debevec, and Ravi Ramamoorthi. Single image portrait relighting. *CoRR*, abs/1905.00824, 2019. 1, 2, 3, 4, 6, 7, 8
- [29] Tiancheng Sun, Zexiang Xu, Xiuming Zhang, Sean Ryan Fanello, Christoph Rhemann, Paul E. Debevec, Yun-Ta Tsai, Jonathan T. Barron, and Ravi Ramamoorthi. Light stage super-resolution: Continuous high-frequency relighting. *CoRR*, abs/2010.08888, 2020. 1, 2, 3, 4
- [30] Yifan Wang, Aleksander Holynski, Xiuming Zhang, and Xuaner Zhang. Sunstage: Portrait reconstruction and relighting using the sun as a light stage. In *Proceedings of the IEEE/CVF Conference on Computer Vision and Pattern Recognition*, pages 20792–20802, 2023. 3
- [31] Zhibo Wang, Xin Yu, Ming Lu, Quan Wang, Chen Qian, and Feng Xu. Single image portrait relighting via explicit multiple reflectance channel modeling. *ACM Trans. Graph.*, 39(6), 2020. 2, 3
- [32] Yu-Ying Yeh, Koki Nagano, Sameh Khamis, Jan Kautz, Ming-Yu Liu, and Ting-Chun Wang. 41(6):1–21, 2022. 2
- [33] Yu-Ying Yeh, Koki Nagano, Sameh Khamis, Jan Kautz, Ming-Yu Liu, and Ting-Chun Wang. Learning to relight portrait images via a virtual light stage and synthetic-to-real adaptation. *ACM Transactions on Graphics (TOG)*, 2022. 2, 3
- [34] Longwen Zhang, Qixuan Zhang, Minye Wu, Jingyi Yu, and Lan Xu. Neural video portrait relighting in real-time via consistency modeling, 2021. 1, 2, 3, 6, 7
- [35] Richard Zhang, Phillip Isola, Alexei A. Efros, Eli Shechtman, and Oliver Wang. The unreasonable effectiveness of deep features as a perceptual metric. *CoRR*, abs/1801.03924, 2018. 7
- [36] R. Zhang, P. Isola, A. A. Efros, E. Shechtman, and O. Wang. The unreasonable effectiveness of deep features as a perceptual metric. In *2018 IEEE/CVF Conference on Computer Vision and Pattern Recognition (CVPR)*, pages 586–595, Los Alamitos, CA, USA, 2018. IEEE Computer Society. 5, 7
- [37] Xuaner Zhang, Jonathan T. Barron, Yun-Ta Tsai, Rohit Pandey, Xiuming Zhang, Ren Ng, and David E. Jacobs. Portrait shadow manipulation. 2020. 1
- [38] Xiuming Zhang, Sean Ryan Fanello, Yun-Ta Tsai, Tiancheng Sun, Tianfan Xue, Rohit Pandey, Sergio Orts-Escolano, Philip L. Davidson, Christoph Rhemann, Paul E. Debevec, Jonathan T. Barron, Ravi Ramamoorthi, and William T. Freeman. Neural light transport for relighting and view synthesis. *CoRR*, abs/2008.03806, 2020. 2, 3
- [39] Hao Zhou, Sunil Hadap, Kalyan Sunkavalli, and David Jacobs. Deep single-image portrait relighting. In *2019 IEEE/CVF International Conference on Computer Vision (ICCV)*, pages 7193–7201, 2019. 1, 2, 4
- [40] Jun-Yan Zhu, Taesung Park, Phillip Isola, and Alexei A Efros. Unpaired image-to-image translation using cycle-consistent adversarial networks. In *Computer Vision (ICCV), 2017 IEEE International Conference on*, 2017. 5

# Personalized Video Relighting With an At-Home Light Stage

## Supplementary Material

### A. Overview of Appendices

Our appendices contain

#### Temporal Consistency (Sec. B)

- In Fig. 7, we compare the temporal changes in skip-connected features between our method and the approaches by [23, 28]. Additionally, we demonstrate that the use of the LCFN module contributes to improved temporal consistency, showing smaller differences in feature space. (Sec. B.1)
- We provide Fig. 1 in video ‘main.mp4’ (Sec. B.2).
- We present video ‘compare.mp4’ demonstrating that our method exhibits greater temporal consistency compared to the approaches of [23, 28] (Sec. B.3).

#### Image Comparison (Sec. C)

- Additional examples of visual comparisons shown in Fig. 4 are demonstrated with the LSYD dataset in Fig. 8, and the OLAT dataset in Fig. 9.
- In Tab. 4, we present a quantitative comparison illustrating the performance improvements brought about by our LCFN and monitor prediction modules. The supporting visual results can be observed in Fig. 10.
- Additional instances of the visual comparison in real-world scenarios, as depicted in Fig. 5, are displayed in Fig. 11.

### B. Temporal Consistency

#### B.1. Feature Difference

In Fig. 7, as evident, the sharp spikes in values occur when  $L_{src}$  undergoes significant changes. In such cases, the difference in skip-connected features is larger compared to scenarios where  $L_{src}$  experiences have small variations. These substantial differences in feature values contribute to temporal inconsistency. Regardless of the magnitude of the change in  $L_{src}$ , our objective is to transmit only the shape and characteristics of the portrait through skip-connected features, without the information about the reflection of light on the face. Therefore, to minimize this difference, we demonstrate that by employing light conditioned feature normalization (LCFN) and delighting the features, we can enhance temporal consistency as shown in red line.

#### B.2. Relit Video

In the ‘main.mp4’ video, we demonstrate how we captured the Light Stage at Your Desk (LSYD) data and showcase the relit results, as described in Fig. 1. From 0 to 7 seconds, we illustrate the process of capturing. The video on the left shows the capturing procedure, with the top-right

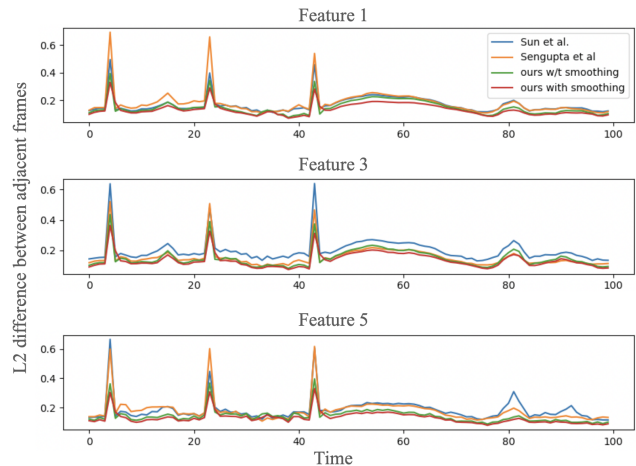


Figure 7. Plots illustrate the L2 distance of skip-connected features (Feature 1, 3, and 5, respectively) between adjacent frames, relighting 100 consecutive portrait images into a single target light. The blue line corresponds to Sun *et al.* [23], the orange line to Sengupta *et al.* [23], the green line to our method, and the red line to our method with LCFN.

corner displaying the portrait video and the bottom featuring the corresponding monitor video. From 7 to 42 seconds, we present the relighting results. On the left side, the input portrait and monitor are displayed, while on the right side, the relit portrait and the target monitor are shown. (Relighting results for different target monitors are presented approximately every 7 seconds.)

#### B.3. Relit Video Comparison

In the ‘compare.mp4’ video, we conduct a comparison with Sun *et al.* [28] and Sengupta *et al.* [23] in terms of temporal consistency, utilizing the ideal ring light as the target light. This video supports two playback speeds (In addition to the original speed video, we provide a 0.5x slowed-down relit video to facilitate a clearer observation of temporal consistency). In the top-left corner is the input portrait, and in the top-right corner is the relit result of ours with LCFN and  $L_{src_{avg}}$ . In the bottom-left corner is Sengupta *et al.* [23]’s relighting result, and in the bottom-right corner is Sun *et al.* [28]’s result. We note that our results are more temporally consistent.

### C. Image Comparison

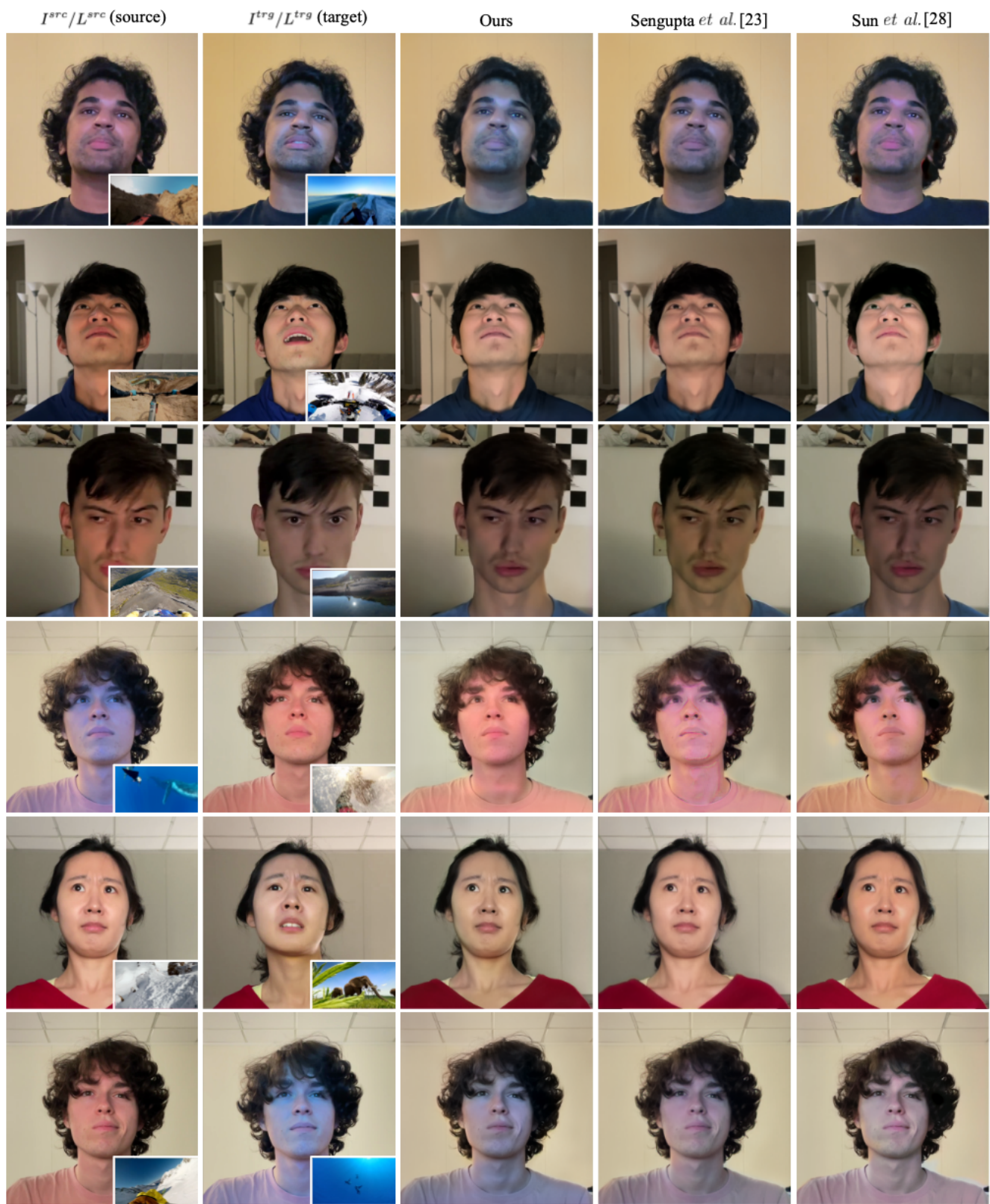


Figure 8. In addition to Fig. 4, we conduct a visual comparison with established relighting techniques [23, 28] using unseen test LSYD data. Our approach (Col. 3) yields notably superior relighting outcomes in contrast to existing methods (Cols 4 and 5).



Figure 9. In addition to Fig. 4, we perform a qualitative comparison with established relighting techniques [23, 28] using unseen test OLAT data [34]. Our method (Col. 3) produces better relighting results compared to existing approaches (Cols 4 and 5).



Figure 10. We present visual evidence supporting the observations outlined in Tab. 4. In comparison with Col. 4 (without the LCFN module), 5 (without  $L_{src}$  prediction), and 6 (without both the LCFN module and  $L_{src}$  prediction), we note that the proposed modules LCFN and  $L_{src}$  prediction exhibit substantial enhancements in our result (Col. 3).

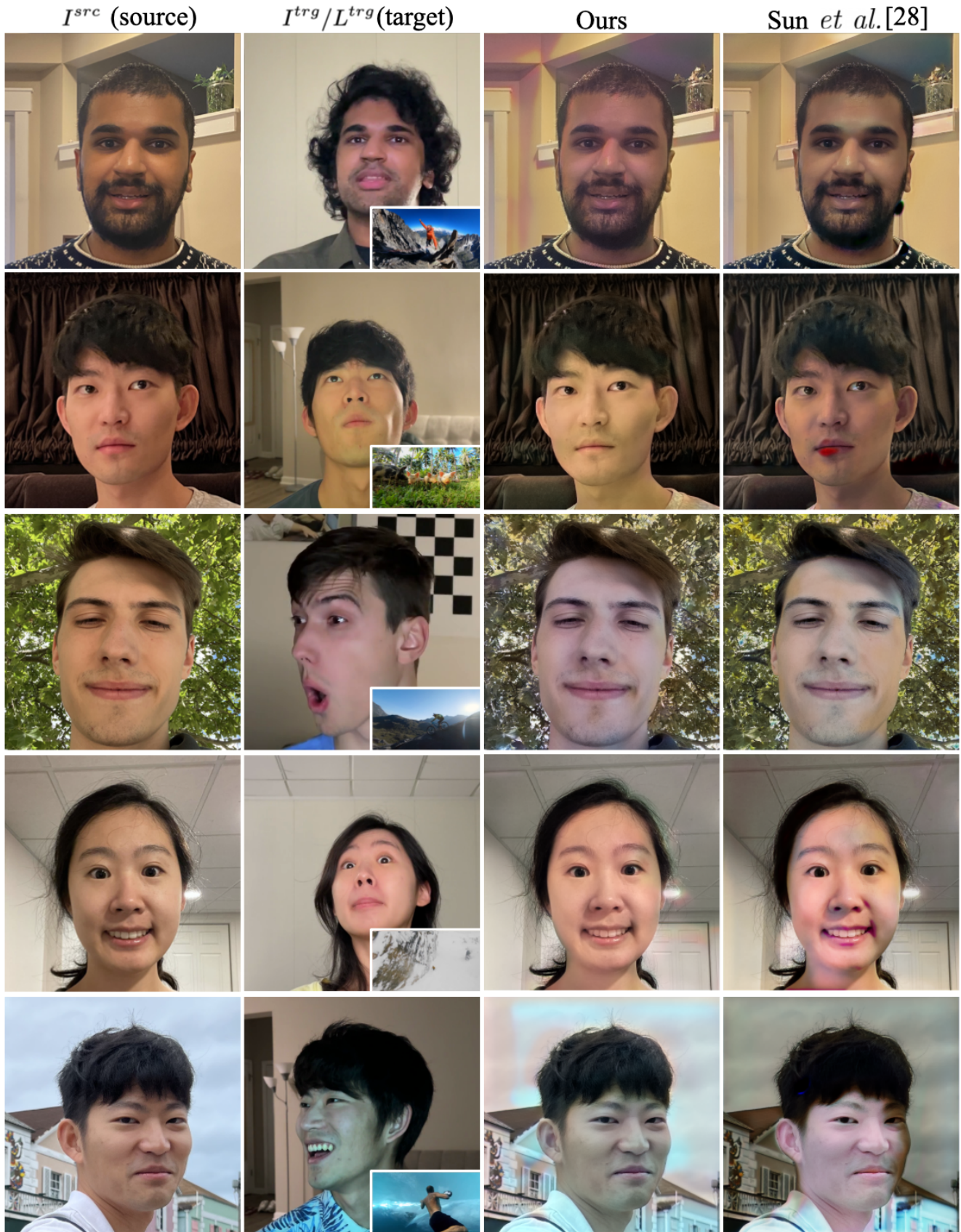


Figure 11. Additional results for Fig. 5